AIMS Mathematics

http://www.aimspress.com/journal/Math

AIMS Mathematics, 11(9): 28078–28096.
DOI: 10.3934/math.20261120
Received: 12 July 2026
Revised: 11 August 2026
Accepted: 14 August 2026
Published: 03 September 2026

Research article

Analytic investigation of the complex nonlinear (2+1)-dimensional Akbota-Myrzakulov-Tolkynay-Zhaidary equation via the new efficient improvement method

Adnan Ahmad Mahmud[1,2,*], Akbota Myrzakul[3,*], Ratbay Myrzakulov[4,6], Hozan Hilmi[5,*], Kalsum Abdulrahman Muhamad[2] and Gulgassyl Nugmanova[6]

[1] Information Technology Department, Tishk International University, Kurdistan Region, Iraq
[2] Department of Mathematics, Faculty of Arts and Sciences, Harran University, 63290, Şanlıurfa, Türkiye
[3] School of Artificial Intelligence and Data Science, Astana IT University, Astana, 010000, Kazakhstan
[4] Ratbay Myrzakulov Eurasian International Centre for Theoretical Physics, Astana, 010009, Kazakhstan
[5] Department of Mathematics, College of Science, University of Sulaimani, Sulaimani 46001, Kurdistan Region, Iraq
[6] Department of Mathematical and Computer Modeling, L. N. Gumilyov Eurasian National University, Astana, 010008, Kazakhstan

* **Correspondence:** Email: mathematic79@yahoo.com, a.myrzakul@astanait.edu.kz, hozan.mhamadhilmi@univsul.edu.iq.

Abstract: This paper investigated a new, complex, triple-integrable system in two spatial dimensions called the Akbota-Myrzakulov-Tolkynay-Zhaidary equation (AMTZE). The AMTZE originates from reducing a larger multi-component geometric spinning system. Aiming to extract some new exact solutions to the updated family of Myrzakulov-type integrable models, we reduce the triple system to a third-order ordinary differential equation (ODE) using a traveling wave transformation. Thereafter, we solved this equation with the modified generalized Kudryashov method. This method uses a rational solution built from an auxiliary Riccati-type equation. A balancing rule controls the form and the shape of the solution. We found several families of exact solutions for the complex-valued functions $q(x, y, t)$, $u(x, y, t)$, and $r(x, y, t)$. These include bright solitons, singular solitons, and mixed wave shapes written in the form of tanh and coth functions. We emphasize that among the six solution families obtained, only Family 1.1 yields real frequencies ω and thus corresponds to standard propagating traveling waves. The remaining five families give imaginary frequencies and represent non-propagating modes. We presented how the free parameters change the height, width, and speed of the waves.

Three-dimensional plots, contour plots, and time-evolution plots made these changes easy to visualize. Our results demonstrated that the method works well on this kind of higher-order, three-dimensional triple system. This work also provided a clear distinction between physically propagating and non-propagating solution branches. All the generated solutions have been verified and satisfy the associated model.

Keywords: AMTZE; Kudryashov method; integrable systems; rational solution; Riccati-type equations
Mathematics Subject Classification: 35C07, 35Q35, 37K10

1. Introduction

Nonlinear partial differential equations (NLPDEs) are fundamental to advanced mathematical physics. They characterize waves in fluids, optical fibers, plasmas, and magnetic elements. Linear equations cannot describe the rich patterns of behavior observed in these systems. Nonlinear systems can. Because of their exact solutions, solitons are of great importance. A soliton is a form of wave that keeps its shape, speed, and energy level as it propagates. It even retains its shape after an impact with another soliton. Identifying new integrable models and generating efficient techniques to solve them are still ongoing research domains.

Mathematics provides a rich collection of new integrable equations. Many systems arise from the motion of standard curves and surfaces in a given space. Ratbay Myrzakulov and his collaborators constructed a large collection of such standardized models. They named several of them after Kazakh given names: Kuralay, Kairat, Akbota, and others. Each of these models is derived from a geometrical flow and admits a Lax pair, ensuring standard integrability [1, 2].

The Kuralay equations are a clear example. They come from the behavior of generated space curves and are essentially identical to generalized Heisenberg ferromagnetic and nonlinear Schrödinger-type systems [3, 4]. Their soliton solutions have been generated using the Hirota bilinear, Riccati-Bernoulli and Bäcklund methods [5], modified exponential rational function method [6], modified auxiliary equation, and Sardar sub-equation approaches [7]. Other studies focused on bifurcation and chaos [8], Bernoulli sub-equation function method and the Khater-II method [9], the modified expansion method and the new extended auxiliary equation method [10], and complete qualitative behavior [11]. Additional work simplified the Kuralay system to M-fractional form and solved it with some analytically algorithms such as the extended sinh-Gordon equation expansion scheme and the generalized Kudryashov scheme [12], while additional soliton kinds were reported [13].

The Akbota equation is a second type of integrable equation and is the closest relative of the model studied here. It is a Heisenberg ferromagnetic-type equation corresponding to the physics of curves and surfaces. Its conservation laws, Jacobi elliptic solutions, and modulation instability were studied in [14]. Its dynamical wave pattern was evaluated by Kong and Guo [15]. Soliton solutions were constructed utilizing the generalized projective Riccati equation procedure, the Sardar sub-equation approach, and the (G'/G^2)-expansion method [16], and later with fractional forms [17, 18]. A closely related model, the Akbota–Gudekli–Kairat–Zhaidary equation, was addressed with the

(G'/G)-expansion and Paul-Painlevé techniques [19], constructing on the more general Myrzakulov-Lakshmanan family [20].

The Kairat models form a third classification. They were demonstrated with a proof of geometric and measurement equivalence between the Kairat-I and Kairat-II equations [21]. Later work developed optical soliton solutions for the Kairat-X equation [22], the extended rational sinh-cosh method, and the modified extended tanh-function method for constructing traveling wave solutions to the (2+1)-dimensional integro-differential Konopelchenko-Dubrovsky equation employed in [23], the analysis of the fractional Kairat-X equation computationally derived in [24], the extension of the Kairat-II and Kairat-X models to (3+1) dimensions, identifying Painlevé integrability, lump solutions, and breather waves in [25].

The AMTZE examined in this paper belongs to this family of mathematically motivated, multi-component integrable systems. It extends the two-dimensional spatial framework and higher-order cross-derivative coupling typical to these models. Like its cousins, it admits a zero-curvature (Lax pair) expression, an infinite set of conservation laws, Darboux and Bäcklund transformations, and measure equivalents to other well-known systems, including the Wu-Zhang system. The Wu-Zhang system itself has been addressed using the generalized Kudryashov method [26] and the first integral procedure under a conformable time-fractional derivative [27].

Recent developments in mathematical physics have greatly advanced our understanding of nonlinear wave phenomena, with several classical methods being refined to solve integrable models. For instance, soliton dynamics were analyzed for the (3+1)-dimensional Gardner-Kadomtsev-Petviashvili model to describe pulse propagation in single-mode optical fibers [28]. In a related study, the (2+1)-dimensional integro-differential Jaulent-Miodek equation was investigated to derive new exact and analytic traveling wave solutions [29]. Building on these efforts, a straightforward yet efficient semi-analytic method was developed to characterize solutions for two significant mathematical models under both fractional and non-fractional frameworks [30]. The (2+1)-dimensional Novikov-Veselov system of equations was likewise examined to reveal its dynamical behavior and underlying soliton solutions [31]. To extend these computational frameworks further, an efficacious improvement to the Anuj transformation method was proposed for solving higher-order fractional differential equations with constant coefficients [32]. Finally, a generalized Hietarinta-type equation was explored through an effective traveling wave transformation to uncover additional exact solution structures [33]. Together, these studies demonstrate the growing power of analytical and semi-analytical methods for extracting and controlling the behavior of complex nonlinear systems.

Recently, some latest findings have been reported for soliton equations and their applications. Yu and Yu [34] utilized the Hirota bilinear method to extract non-autonomous soliton solutions for the (2+1)-dimensional higher-order nonlinear Schrödinger equation with variable coefficients. Additional recent studies have explored M-fractional Kudryashov-type equations [35] and soliton dynamics in various integrable models [36]. The continued exploration of these models helps to uncover new physical phenomena and mathematical structures.

The complex AMTZE is a newly constructed example of these integrable systems. Developed from geometric and physical fundamentals, it is a triple multi-component framework that operates as an essential research facility for soliton mathematics. Formally, after a standard reduction, the model generates the following multi-component system [37]:

$$iq_t + \beta q q_y - u q_x - i\beta r_y = 0, \tag{1.1}$$

$$ir_t + \beta r q_y - u r_x - \frac{\beta}{4\alpha} q_{xxy} = 0, \tag{1.2}$$

$$u_x + \frac{\beta}{2} q_y = 0. \tag{1.3}$$

Equations (1.1)–(1.3) represent the AMTZE system. Here, $q(x, y, t)$, $u(x, y, t)$, and $r(x, y, t)$ are complex-valued functions that indicate the corresponding state variable areas in two space dimensions (x, y) over time t, whereas α and β are parameter values. These equations describe wave dynamics in two spatial dimensions with nonlinear coupling among the three fields. The system captures complex interactions that cannot be described by simpler one-dimensional models. This model, in its non-complex form, has recently been studied using the modified Sardar method [38]. Recent advances have also focused on nonlocal and variable-coefficient integrable systems. Zhou and Yu [39] investigated a generalized nonlocal nonlinear Schrödinger equation, constructing space-time shifted soliton solutions and analyzing their interaction dynamics via the Hirota bilinear method. Liu et al. [40] studied the variable-coefficient Melnikov system, deriving soliton solutions and examining long-time asymptotics using the nonlinear steepest descent method. Zhang et al. [41] explored the variable-coefficient Davey-Stewartson II equation, analyzing soliton interaction dynamics, long-time asymptotics, and modulation instability in nonlinear media.

From an integrability viewpoint, the AMTZE shows all fundamental characteristics of completely integrable systems. Its framework allows for a zero-curvature condition via a Lax pair, expressing an infinite number of conservation laws, a Hamiltonian framework, Darboux/Bäcklund transformations, and measure equivalents to other commonly used equations. In structural terms, the equation models deep-water wave dynamics, nonlinear optics in atypical scattering media, and the differential shape of moving curves and surfaces in polarized systems. The multi-directional components (x, y) allow rich configurations, including bright, dark, rational, periodic, and Jacobi elliptic wave patterns.

To utilize the underlying physical processes of the AMTZE, reliable analytical schemes are essential. Aiming to bypass the limitations of other methods, this study utilizes the modified generalized Kudryashov method.

The fundamental purpose of this paper is to simplify the AMTZE system using a traveling wave transformation and address the resulting ordinary differential system via the modified generalized Kudryashov method. We demonstrate newly identified closed-form exact solutions as well as their mathematical configurations through 3D profiles and contour standard distributions, providing meaningful insight into the localized wave fields and motion diffusion dynamics of the AMTZE model.

The structure of this paper is as follows: Section 1 includes the introduction and a review of the literature on related works. Section 2 provides an overview of the utilized methodology. Section 3 is specialized for transforming the examined model into an ODE. The application of the implemented technique for the investigated model is outlined in Section 4. The results and discussion section has been addressed in Section 5. Final conclusive comments and recommendations have been incorporated in Section 6.

2. Methodology overview

The main workflow of the implemented method can be organized into four initial stages, as demonstrated.

Step 1: Wave transformation

We proceed with a multidimensional nonlinear partial differential equation (NPDE) that takes on the following form:

$$F(u, u_x, u_y, u_{xx}, u_{yy}, u_t, u_{xt}, \cdots) = 0, \tag{2.1}$$

here, u depends heavily on space and time variables. We streamline this form using a traveling wave parameter ζ:

$$u(x, y, t) = H(\zeta), \quad \zeta = c_1 x + c_2 y - \lambda t. \tag{2.2}$$

The terms c_1, c_2, and λ represent arbitrary, non-zero parameters. Substituting this wave variable into our original model transforms it into a nonlinear ODE:

$$E(H, H', H'', \cdots) = 0 . \tag{2.3}$$

Step 2: Suggesting the solution form

We suppose the solution follows a certain rational structure. We express the solution as a corresponding ratio of finite series:

$$H(\zeta) = \frac{\sum_{i=0}^{p} a_i [W(\zeta)]^i}{\sum_{j=0}^{q} b_j [W(\zeta)]^j}. \tag{2.4}$$

The numerators and denominators terminate at integers p and q. The function $W(\zeta)$ is controlled by the following derivative rule:

$$W' = 1 + 2\rho W + (\rho^2 - 1) W^2, \tag{2.5}$$

where ρ is a constant parameter with $\rho \notin \{0, 1, -1\}$.

Remark 2.1. *We could find exact solutions for those left-out values. If $\rho = 0$, the exact solution simplifies to*

$$W = \tanh(A + \zeta). \tag{2.6}$$

Similarly, if $\rho = \mp 1$, the exact solutions become:

$$W = 1 + \Gamma e^{-\zeta} \quad \text{and} \quad W = -1 + \Gamma e^{\zeta}. \tag{2.7}$$

In these cases, Γ represents a free parameter.

We plug our main recommended structure back into our ODE. Grouping similar terms yields a polynomial expression:

$$H(W(\zeta)) = \rho_\tau [W(\zeta)]^\tau + \cdots + \rho_1 W(\zeta) + \rho_0 = 0. \tag{2.8}$$

To find the upper limits p and q, we employ homogeneous balancing, comparing the highest order with the highest degree.

Step 3: Setting up and solving the system

To make the polynomial equation true for all cases, we extract its coefficients. We set each collected coefficient to zero:

$$\rho_r = 0, \quad r = 0, \cdots, \tau. \tag{2.9}$$

This step creates a full set of algebraic equations. Solving this algebraic system fixes our unknown parameters. Once we find these values, we can rebuild the solution structure for our studied model.

Step 4: Constructing final solutions

The final procedure involves analyzing the primary auxiliary equation. The solution behavior can be illustrated via the following forms:

$$W(\zeta) = \frac{\tanh(\zeta)}{1 - \rho\tanh(\zeta)} \qquad \text{or simply} \qquad W(\zeta) = \frac{1}{-\rho + \coth(\zeta)}. \tag{2.10}$$

These two forms are mathematically equivalent since $\coth(\zeta) = 1/\tanh(\zeta)$. They represent the same solution expressed differently. Using these generated profiles with our parameter values gives us the final solutions for the initial model.

3. Traveling wave transformation

To reduce the initial system into an ODE, we define the transformations:

$$q(x, y, t) = Q(\xi), \quad u(x, y, t) = U(\xi), \quad r(x, y, t) = R(\xi), \tag{3.1}$$

and the wave coordinate ξ:

$$\xi = kx + ly - \omega t, \tag{3.2}$$

where k, l represent the wave numbers along the space dimensions and ω is the wave frequency. The partial derivative operators are converted into ordinary derivative operators subsequently concerning ξ. After substituting into Eqs (1.1)–(1.3), the resulting system of triple ODEs is generated:

$$-i\omega Q' - kUQ' + \beta lQQ' - i\beta lR' = 0, \tag{3.3}$$

$$-i\omega R' - kUR' + \beta lRQ' - \frac{\beta k^2 l}{4\alpha}Q''' = 0, \tag{3.4}$$

$$kU' + \frac{\beta l}{2}Q' = 0, \tag{3.5}$$

where the primes ($'$) denote differentiation with respect to ξ. We follow the standard reduction procedure:

Step 1: By integrating Eq (3.5) with respect to ξ, and for localized solitary wave boundaries, setting the constant of integration to zero, we obtain:

$$U(\xi) = -\frac{\beta l}{2k}Q(\xi). \tag{3.6}$$

Step 2: By substituting (3.6) back into (3.3), simplifying, and integrating once (with zero integration constant), we obtain:

$$R(\xi) = -\frac{\omega}{\beta l} Q(\xi) - i\frac{3}{4} Q(\xi)^2. \tag{3.7}$$

Differentiating (3.7) with respect to ξ provides:

$$R'(\xi) = -\frac{\omega}{\beta l} Q'(\xi) - i\frac{3}{2} Q(\xi) Q'(\xi). \tag{3.8}$$

Step 3: By substituting the profiles for $U(\xi)$, $R(\xi)$, and $R'(\xi)$ into (3.4), and expanding and combining terms, we obtain:

$$\frac{i\omega^2}{l\beta} Q' - 3\omega Q Q' - i\frac{3\beta l}{2} Q^2 Q' - \frac{l\beta k^2}{4\alpha} Q''' = 0. \tag{3.9}$$

Step 4: Integrating this resulting equation once more with respect to ξ produces the simplified, second-order non-linear ODE for $Q(\xi)$. For classic analytic solutions such as solitons, the integration constant is chosen as 0, yielding:

$$\frac{l\beta k^2}{4\alpha} \frac{d^2 Q}{d\xi^2} - \frac{i\omega^2}{l\beta} Q + \frac{3\omega}{2} Q^2 + i\frac{l\beta}{2} Q^3 = 0\cdot \tag{3.10}$$

4. Applications of the modified generalized Kudryashov method

Considering the balancing principles in Eq (3.10) between $\frac{d^2 Q}{d\xi^2}$, $Q^3(\xi)$, we obtain a formula for p and q as follows:

$$p = q + 1. \tag{4.1}$$

Equation (4.1) produces subsequent instances for the positive integers that already exist.

Family 1. In Eq (4.1), if $q = 1$ and $p = 2$, then Eq (2.4) simplifies to:

$$Q(\xi) = \frac{\sigma_2 \phi^2 + \sigma_1 \phi + \sigma_0}{\theta_1 \phi + \theta_0}. \tag{4.2}$$

Here, we use ϕ interchangeably with $W(\xi)$ for convenience in the algebraic manipulation. Eq (2.5) is considered, hence:

$$\begin{aligned} Q'(\xi) &= \left(\left(\rho^2 - 1\right)\phi^2 + 2\rho\phi + 1\right)\left(\frac{2\sigma_2\phi + \sigma_1}{\theta_1\phi + \theta_0} - \frac{\theta_1\left(\sigma_2\phi^2 + \sigma_1\phi + \sigma_0\right)}{\left(\theta_1\phi + \theta_0\right)^2}\right) \\ &= \frac{\Phi(\mathscr{T})}{\Psi(\mathscr{T})}, \end{aligned} \tag{4.3}$$

and there should be at least $\sigma_2 \neq 0, \theta_1 \neq 0$. It is clear that:

$$Q''(\xi) = \frac{\Psi(\mathscr{T})\Phi^{'}(\mathscr{T}) - \Phi(\mathscr{T})\Psi^{'}(\mathscr{T})}{(\Psi(\mathscr{T}))^2}. \tag{4.4}$$

By substituting Eqs (4.2)–(4.4) into Eq (3.10), we obtain the following algebraic system of equations by setting all coefficients of the same powers of $\mathscr{T}^i$ to zero for $i = 0, 1, 2, \cdots, 7$.

$$\sum_{i=0}^{7} \text{coefficients of } (Q(\xi))^i = 0. \tag{4.5}$$

The following sub-cases are established through the solution of the system given in Eq (4.5).

Family 1.1. The obtained parameters are:

$$\begin{aligned} k &= \frac{(-1)^{3/4}\sqrt{\alpha}\sigma_2}{\sqrt{(\rho^2-1)^2\theta_1^2}}; l = \frac{\left(\rho^2-1\right)\theta_1\omega}{\sqrt{2}\beta\sigma_2}; \theta_0 = \frac{\rho\theta_1}{\rho^2-1};\\ \sigma_0 &= \frac{\left(\rho^2+i\sqrt{2}\rho-1\right)\sigma_2}{(\rho^2-1)^2}; \sigma_1 = \frac{\left(2\rho+i\sqrt{2}\right)\sigma_2}{\rho^2-1}. \end{aligned} \tag{4.6}$$

This family yields real ω and thus represents standard propagating waves.

By using (4.6), the next solution is constructed:

$$\begin{aligned} q_{1,1} &= \frac{\sigma_2\left(-1+\left(\frac{\rho^2}{-\coth(\mathscr{A})-\rho}-\frac{1}{-\coth(A)-\rho}+\rho+i\sqrt{2}\right)\left(\frac{\rho^2-1}{-\coth(\mathscr{A})-\rho}+\rho\right)\right)}{(\rho^2-1)^2\theta_1\left(\frac{1}{-\coth(\mathscr{A})-\rho}+\frac{\rho}{\rho^2-1}\right)},\\ u_{1,1} &= \frac{\sqrt[4]{-1}\omega\sqrt{(\rho^2-1)^2\theta_1^2}\left(-1+\left(\frac{\rho^2}{-\coth(\mathscr{A})-\rho}-\frac{1}{-\coth(\mathscr{A})-\rho}+\rho+i\sqrt{2}\right)\left(\frac{\rho^2-1}{-\coth(\mathscr{A})-\rho}+\rho\right)\right)}{2\sqrt{2}\sqrt{\alpha}(\rho^2-1)\sigma_2\left(\frac{1}{-\coth(\mathscr{A})-\rho}+\frac{\rho}{\rho^2-1}\right)},\\ r_{1,1} &= -\frac{\sigma_2\left(3i\sigma_2\omega\left(-1+\left(\frac{\rho^2}{-\coth(\mathscr{A})-\rho}-\frac{1}{-\coth(\mathscr{A})-\rho}+\rho+i\sqrt{2}\right)\left(\frac{\rho^2-1}{-\coth(\mathscr{A})-\rho}+\rho\right)\right)^2\right)}{\left(2\sqrt{2}(\rho^2-1)\theta_1\omega\right)\left(\sqrt{2}(\rho^2-1)^3\theta_1\left(\frac{1}{-\coth(\mathscr{A})-\rho}+\frac{\rho}{\rho^2-1}\right)^2\right)}\\ &\quad-\frac{\sigma_2\left(4\sigma_2\omega\left(-1+\left(\frac{\rho^2}{-\coth(\mathscr{A})-\rho}-\frac{1}{-\coth(\mathscr{A})-\rho}+\rho+i\sqrt{2}\right)\left(\frac{\rho^2-1}{-\coth(\mathscr{A})-\rho}+\rho\right)\right)\right)}{\left(2\sqrt{2}(\rho^2-1)\theta_1\omega\right)\left((\rho^2-1)^2\theta_1\left(\frac{1}{-\coth(\mathscr{A})-\rho}+\frac{\rho}{\rho^2-1}\right)\right)}, \end{aligned} \tag{4.7}$$

where

$$\mathscr{A} = t\omega - \frac{(-1)^{3/4}\sqrt{\alpha}\sigma_2 x}{\sqrt{(\rho^2-1)^2\theta_1^2}} - \frac{\left(\rho^2-1\right)\theta_1 y\omega}{\sqrt{2}\beta\sigma_2}.$$

We set $\sigma_2 = \frac{1}{6}, \theta_1 = \frac{1}{5}, \rho = \frac{5}{4}, y = \frac{2}{3}, \beta = \frac{3}{4}, \omega = \frac{1}{2}, \alpha = \frac{3}{4}$, $-10 \leq x \leq 10$, and $0 \leq t \leq 10$, and the structure of $q_{1,1}$ in solution (4.7) is illustrated by the Figures 1–4 .

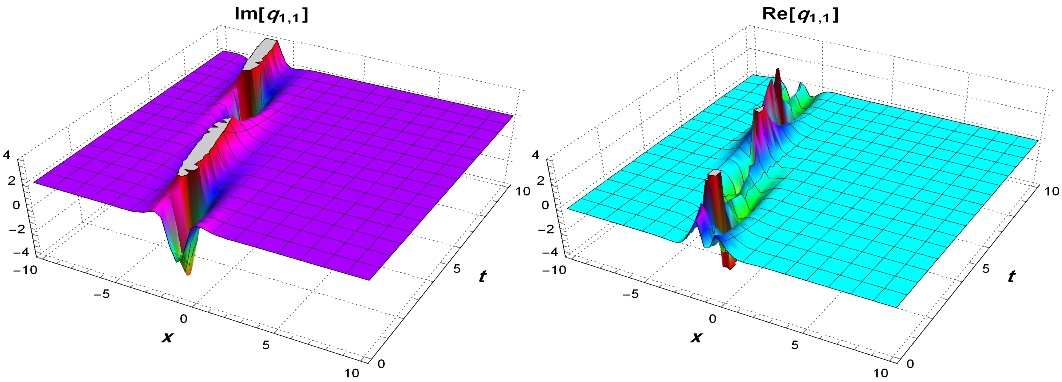

(a) Im$\{q_{1,1}\}$ in (4.7) **(b)** Re$\{q_{1,1}\}$ in (4.7)

Figure 1. Profile of $q_{1,1}$ in three-dimensional figures.

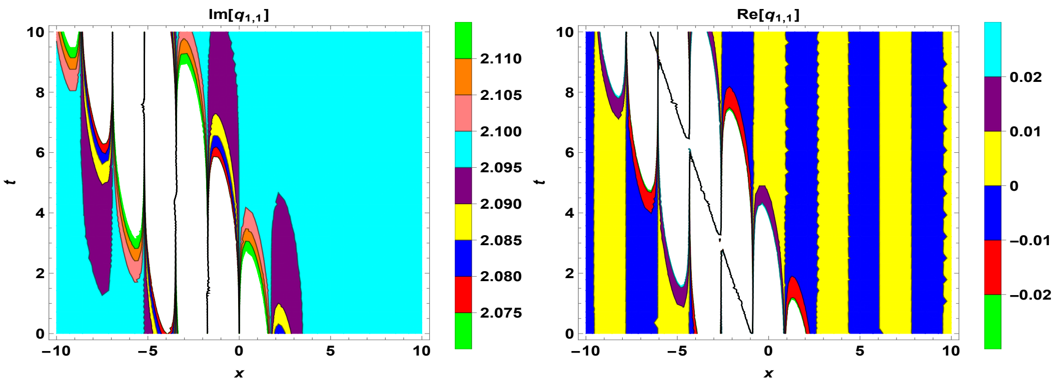

(a) Im$\{q_{1,1}\}$ in (4.7) **(b)** Re$\{q_{1,1}\}$ in (4.7)

Figure 2. Profile of $q_{1,1}$ in two-dimensional contour surface plots.

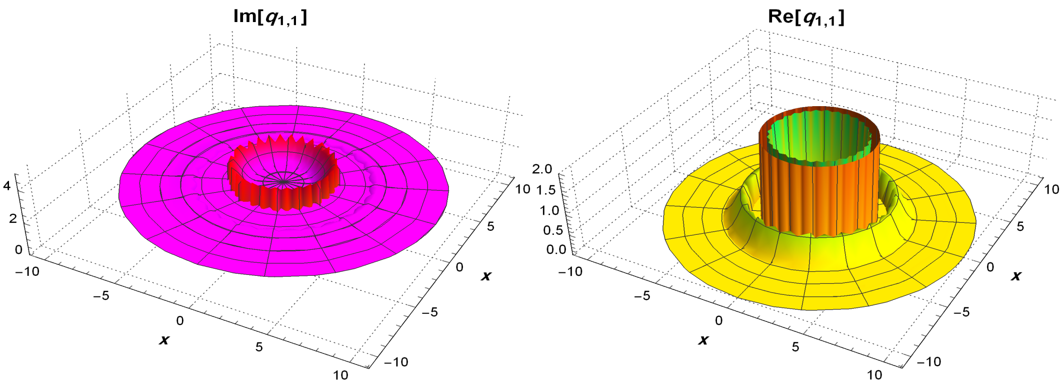

(a) Im$\{q_{1,1}\}$ in (4.7) **(b)** Re$\{q_{1,1}\}$ in (4.7)

Figure 3. Profile of $q_{1,1}$ in 3-dimensional revolving figures.

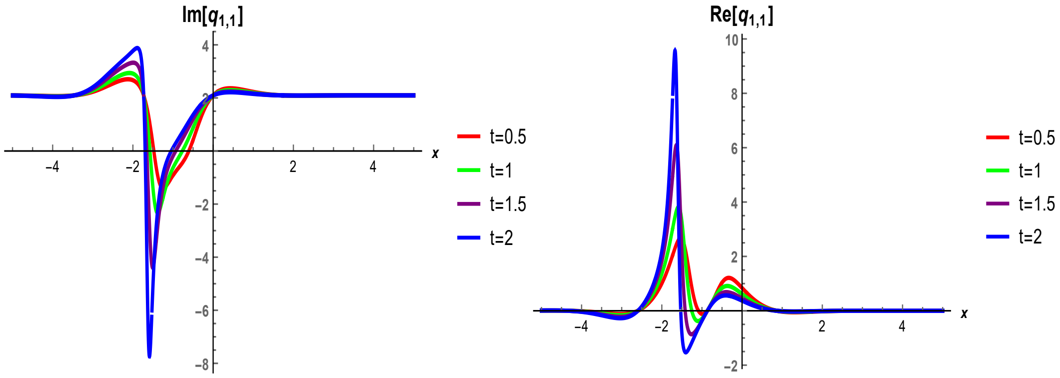

(a) Im$\{q_{1,1}\}$ in (4.7) **(b)** Re$\{q_{1,1}\}$ in (4.7)

Figure 4. Profile of $q_{1,1}$ in two-dimensional time-evolution graphs, where the values of t are presented in the legend.

Family 1.2. The obtained parameters are:

$$\omega = \frac{i\beta l\sigma_2}{(\rho^2-1)\,\theta_1}; \theta_0 = \theta_1\left(\frac{\sigma_1}{\sigma_2} - \frac{1}{\rho+1}\right); \sigma_0 = \frac{(\rho+1)\sigma_1 - \sigma_2}{(\rho+1)^2}; \alpha = \frac{i\left(\rho^2-1\right)^2\theta_1^2 k^2}{\sigma_2^2}. \tag{4.8}$$

Here, ω is purely imaginary, which means the wave variable $\xi = kx + ly - \omega t$ has an imaginary time component. This leads to exponential growth or decay in time rather than standard propagating wave behavior. Such solutions represent non-propagating or unstable modes. From (4.8), the following solution has been obtained:

$$\begin{aligned}
q_{1,2} &= \frac{\sigma_2\left(-\frac{1}{\rho+1} + \frac{1}{1-\rho\tanh\left(kx-\frac{i\beta l\sigma_2 t}{(\rho^2-1)\theta_1}+ly\right)}\right)}{\rho\theta_1},\\
u_{1,2} &= \frac{\beta l\sigma_2\left(\frac{1}{\rho+1} + \frac{1}{-1+\rho\tanh\left(kx-\frac{i\beta l\sigma_2 t}{(\rho^2-1)\theta_1}+ly\right)}\right)}{2\rho\theta_1 k},\\
r_{1,2} &= \frac{i\sigma_2^2\left(1+\tanh\left(kx-\frac{i\beta l\sigma_2 t}{(\rho^2-1)\theta_1}+ly\right)\right)\left(-3\rho+(\rho+3)\tanh\left(kx-\frac{i\beta l\sigma_2 t}{(\rho^2-1)\theta_1}+ly\right)-1\right)}{4(\rho-1)(\rho+1)^2\theta_1^2\left(-1+\rho\tanh\left(kx-\frac{i\beta l\sigma_2 t}{(\rho^2-1)\theta_1}+ly\right)\right)^2}.
\end{aligned} \tag{4.9}$$

Family 1.3. The obtained parameters are:

$$l = -\frac{i\left(\rho^2-1\right)\theta_1\omega}{\beta\sigma_2}; \sigma_1 = \sigma_2\left(\frac{1}{\rho+1} + \frac{\theta_0}{\theta_1}\right); \sigma_0 = \frac{\theta_0\sigma_2}{(\rho+1)\theta_1}; k = \frac{(-1)^{3/4}\sqrt{\alpha}\sigma_2}{\sqrt{\left(\rho^2-1\right)^2\theta_1^2}}. \tag{4.10}$$

This family also yields imaginary ω (non-propagating mode). Utilizing (4.10), one derives the following solution.

$$\begin{aligned} q_{1,3} &= \frac{\sigma_2 \left(-\frac{1}{\rho+1} + \frac{1}{1+\rho \tanh\left(t\omega - \frac{(-1)^{3/4}\sqrt{\alpha}\sigma_2 x}{\sqrt{\left(\rho^2-1\right)^2\theta_1^2}} + \frac{i\left(\rho^2-1\right)\theta_1 y\omega}{\beta\sigma_2} \right)} \right)}{\rho\theta_1}, \\ u_{1,3} &= -\frac{(-1)^{3/4}\left(\rho^2-1\right)\omega\sqrt{\left(\rho^2-1\right)^2\theta_1^2}\left(-\frac{1}{\rho+1} + \frac{1}{1+\rho\tanh(A)} \right)}{2\sqrt{\alpha}\rho\sigma_2}, \\ r_{1,3} &= \frac{i\sigma_2 \left(-\frac{3\left(\rho^2-1\right)\sigma_2\omega\left(-\frac{1}{\rho+1}+\frac{1}{1+\rho\tanh(A)}\right)^2}{\rho^2\theta_1} - \frac{4\sigma_2\omega\left(-\frac{1}{\rho+1}+\frac{1}{1+\rho\tanh(A)}\right)}{\rho\theta_1} \right)}{4\left(\rho^2-1\right)\theta_1\omega}, \end{aligned} \tag{4.11}$$

where

$$A = -\frac{(-1)^{3/4}\sqrt{\alpha}\sigma_2}{\sqrt{\left(\rho^2-1\right)^2\theta_1^2}}x + \frac{i\left(\rho^2-1\right)\theta_1\omega}{\beta\sigma_2}y + \omega t.$$

Family 2. In Eq (4.1), if $q = 2$ and $p = 3$, Eq (2.4) appears as:

$$Q(\xi) = \frac{\sigma_3\phi^3 + \sigma_2\phi^2 + \sigma_1\phi + \sigma_0}{\theta_2\phi^2 + \theta_1\phi + \theta_0}. \tag{4.12}$$

Again, ϕ represents $W(\xi)$ from Eq (2.5), hence:

$$\begin{aligned} Q'(\xi) = &- \frac{\left(\left(\rho^2-1\right)\phi^2 + 2\rho\phi + 1\right)\left((2\theta_2\phi + \theta_1)\left(\sigma_3\phi^3 + \sigma_2\phi^2\sigma_1\phi + \sigma_0\right)\right)}{\left(\theta_2\phi^2 + \theta_1\phi + \theta_0\right)^2} \\ &+ \frac{\left(\left(\rho^2-1\right)\phi^2 + 2\rho\phi + 1\right)\left(3\sigma_3\phi^2 + 2\sigma_2\phi + \sigma_1\right)}{\theta_2\phi^2 + \theta_1\phi + \theta_0} = \frac{\Phi(\xi)}{\Psi(\xi)}, \end{aligned} \tag{4.13}$$

and there should be at least $\sigma_3 \neq 0,\ \theta_2 \neq 0$. Now, one can reach:

$$Q''(\xi) = \frac{\Psi(\xi)\Phi'(\xi) - \Phi(\xi)\Psi'(\xi)}{(\Psi(\xi))^2}. \tag{4.14}$$

By inserting Eqs (4.12)–(4.14) into Eq (2.4), we obtain the following system. By setting all coefficients of the same powers of $\mathscr{T}^i$ to zero, for $i = 0, 1, 2, \cdots, 10$,

$$\sum_{i=0}^{10} \text{coefficients of } (Q(\xi))^i = 0. \tag{4.15}$$

The following sub-cases are created by solving system (4.15).

Family 2.1. The obtained parameters are:

$$\begin{aligned} &\sigma_0 = \frac{(\rho+1)^2\sigma_1 - (\rho+1)\sigma_2 + \sigma_3}{(\rho+1)^3}; k = -\frac{(-1)^{3/4}\sqrt{\alpha}\sigma_3}{\sqrt{\left(\rho^2-1\right)^2\theta_2^2}}; \omega = \frac{i\beta l\sigma_3}{\left(\rho^2-1\right)\theta_2}; \\ &\theta_0 = \frac{\theta_2\left((\rho+1)^2\sigma_1 - (\rho+1)\sigma_2 + \sigma_3\right)}{(\rho+1)^2\sigma_3}; \theta_1 = \theta_2\left(\frac{\sigma_2}{\sigma_3} - \frac{1}{\rho+1}\right). \end{aligned} \tag{4.16}$$

Similar to Family 1.2, ω is purely imaginary here, indicating non-propagating wave behavior. From Eq (4.16), the next solution is attained:

$$
\begin{aligned}
q_{2,1} &= -\frac{\sigma_3}{\rho(\rho+1)\theta_2} - \frac{\sigma_3}{\rho\theta_2\left(-1+\rho\tanh\left(-\frac{i\beta l\sigma_3 t}{(\rho^2-1)\theta_2}+ly-\frac{(-1)^{3/4}\sqrt{\alpha}\sigma_3 x}{\sqrt{\left(\rho^2-1\right)^2\theta_2^2}}\right)\right)},\\
u_{2,1} &= -\frac{\sqrt[4]{-1}\beta l\sqrt{\left(\rho^2-1\right)^2\theta_2^2}}{2\sqrt{\alpha}(\rho+1)\theta_2} + \frac{\sqrt[4]{-1}\beta l\sqrt{\left(\rho^2-1\right)^2\theta_2^2}\tanh\left(-\frac{i\beta l\sigma_3 t}{(\rho^2-1)\theta_2}+ly-\frac{(-1)^{3/4}\sqrt{\alpha}\sigma_3 x}{\sqrt{\left(\rho^2-1\right)^2\theta_2^2}}\right)}{2\sqrt{\alpha}\theta_2\left(-1+\rho\tanh\left(-\frac{i\beta l\sigma_3 t}{(\rho^2-1)\theta_2}+ly-\frac{(-1)^{3/4}\sqrt{\alpha}\sigma_3 x}{\sqrt{\left(\rho^2-1\right)^2\theta_2^2}}\right)\right)},\\
r_{2,1} &= \frac{i(\rho+3)\sigma_3^2}{4(\rho-1)\rho^2(\rho+1)^2\theta_2^2} - \frac{3i\sigma_3^2}{4\rho^2\theta_2^2\left(-1+\rho\tanh\left(-\frac{i\beta l\sigma_3 t}{(\rho^2-1)\theta_2}+ly-\frac{(-1)^{3/4}\sqrt{\alpha}\sigma_3 x}{\sqrt{\left(\rho^2-1\right)^2\theta_2^2}}\right)\right)^2}\\
&\quad - \frac{i(\rho-3)\sigma_3^2}{2(\rho-1)\rho^2(\rho+1)\theta_2^2\left(-1+\rho\tanh\left(-\frac{i\beta l\sigma_3 t}{(\rho^2-1)\theta_2}+ly-\frac{(-1)^{3/4}\sqrt{\alpha}\sigma_3 x}{\sqrt{\left(\rho^2-1\right)^2\theta_2^2}}\right)\right)}.
\end{aligned}
\tag{4.17}
$$

Family 2.2. The obtained parameters are:

$$
\begin{aligned}
&\omega = \frac{i\beta l\sigma_3}{\theta_2-\rho^2\theta_2};\ \alpha = \frac{i\left(\rho^2-1\right)^2\theta_2^2k^2}{\sigma_3^2};\ \theta_1 = \theta_2\left(\frac{1}{1-\rho}+\frac{\sigma_2}{\sigma_3}\right);\\
&\sigma_0 = \frac{\theta_0\sigma_3}{(\rho-1)\theta_2};\ \sigma_1 = \sigma_3\left(\frac{\theta_0}{\theta_2}-\frac{1}{(\rho-1)^2}\right)+\frac{\sigma_2}{\rho-1}.
\end{aligned}
\tag{4.18}
$$

Again, this family has imaginary ω, yielding non-propagating modes. With the given coefficients in Eq (4.18), the following solution has been obtained:

$$
\begin{aligned}
q_{2,2} &= \frac{\sigma_3\left(\frac{1}{\rho-1}+\frac{1}{1-\rho\tanh\left(kx+\frac{i\beta l\sigma_3 t}{\left(\rho^2-1\right)\theta_2}+ly\right)}\right)}{\rho\theta_2},\\
u_{2,2} &= -\frac{\beta l\sigma_3\left(\frac{1}{\rho-1}+\frac{1}{1-\rho\tanh\left(kx+\frac{i\beta l\sigma_3 t}{\left(\rho^2-1\right)\theta_2}+ly\right)}\right)}{2\rho\theta_2 k},\\
r_{2,2} &= \frac{i(\rho-3)\sigma_3^2}{4(\rho-1)^2\rho^2(\rho+1)\theta_2^2} - \frac{3i\sigma_3^2}{4\rho^2\theta_2^2\left(-1+\rho\tanh\left(kx+\frac{i\beta l\sigma_3 t}{(\rho^2-1)\theta_2}+ly\right)\right)^2}\\
&\quad + \frac{i(\rho+3)\sigma_3^2}{2(\rho-1)\rho^2(\rho+1)\theta_2^2\left(-1+\rho\tanh\left(kx+\frac{i\beta l\sigma_3 t}{(\rho^2-1)\theta_2}+ly\right)\right)}.
\end{aligned}
\tag{4.19}
$$

Family 2.3. The obtained parameters are:

$$\begin{aligned}
\alpha &= \frac{i\left(\rho^2-1\right)^2\theta_2^2k^2}{\sigma_3^2};\sigma_1 = \frac{\theta_1\sigma_3}{(\rho+1)\theta_2}+(\rho+1)\sigma_0;\\
\sigma_2 &= \sigma_3\left(\frac{1}{\rho+1}+\frac{\theta_1}{\theta_2}\right);\theta_0 = \frac{(\rho+1)\theta_2\sigma_0}{\sigma_3};\omega = \frac{i\beta l\sigma_3}{\left(\rho^2-1\right)\theta_2}.
\end{aligned} \tag{4.20}$$

This family also gives imaginary ω (non-propagating mode). Utilizing (4.20), we derive the following solution.

$$\begin{aligned}
q_{2,3} &= -\frac{\sigma_3\left(1+\coth\left(kx-\frac{i\beta l\sigma_3 t}{(\rho^2-1)\theta_2}+ly\right)\right)}{(\rho+1)\theta_2\left(\rho-\coth\left(kx-\frac{i\beta l\sigma_3 t}{(\rho^2-1)\theta_2}+ly\right)\right)},\\
u_{2,3} &= \frac{\beta l\sigma_3\left(1+\coth\left(kx-\frac{i\beta l\sigma_3 t}{(\rho^2-1)\theta_2}+ly\right)\right)}{2(\rho+1)\theta_2 k\left(\rho-\coth\left(kx-\frac{i\beta l\sigma_3 t}{(\rho^2-1)\theta_2}+ly\right)\right)},\\
r_{2,3} &= \frac{\frac{4i\beta l\sigma_3^2\left(1+\coth\left(kx-\frac{i\beta l\sigma_3 t}{(\rho^2-1)\theta_2}+ly\right)\right)}{(\rho+1)(\rho^2-1)\theta_2^2\left(\rho-\coth\left(kx-\frac{i\beta l\sigma_3 t}{(\rho^2-1)\theta_2}+ly\right)\right)}-\frac{3i\beta l\sigma_3^2\left(1+\coth\left(kx-\frac{i\beta l\sigma_3 t}{(\rho^2-1)\theta_2}+ly\right)\right)^2}{(\rho+1)^2\theta_2^2\left(\rho-\coth\left(kx-\frac{i\beta l\sigma_3 t}{(\rho^2-1)\theta_2}+ly\right)\right)^2}}{4\beta l}.
\end{aligned} \tag{4.21}$$

Remark 4.1. *We have considered only two families, each with three sub cases. For different values of p and q, researchers can consider many different cases in order to obtain some other sets of solutions. This is one of the significant features of the applied method.*

5. Results and discussion

The six subfamilies derived in this article address both the tanh-type branch characterized by Family 1 and the coth rational branch characterized by Family 2 of the solutions to the given auxiliary equation. Together they give a sufficiently complete illustration of the wave shapes that the complex AMTZE can conform to.

Categorization of solution families. A crucial distinction must be made regarding the physical nature of the obtained solutions. The parameter ω (wave frequency) determines whether a solution represents a propagating wave or a non-propagating mode (Table 1).

Table 1. Categorization of solution families by frequency type and physical behavior.

Family	Frequency ω	Behavior	Type
Family 1.1	Real	Smooth, bounded	Propagating wave
Family 1.2	Imaginary	Exponential growth/decay	Non-propagating mode
Family 1.3	Imaginary	Exponential growth/decay	Non-propagating mode
Family 2.1	Imaginary	Exponential growth/decay	Non-propagating mode
Family 2.2	Imaginary	Exponential growth/decay	Non-propagating mode
Family 2.3	Imaginary	Exponential growth/decay	Non-propagating mode

Only Family 1.1 yields real ω and thus corresponds to standard propagating waves. The remaining families, while having mathematically valid solutions to the reduced ODE, represent non-propagating modes due to imaginary frequencies.

Wave shapes. Family 1.1 provides a solution constructed from $\coth(A)$, and its imaginary and real parts both show high, thin, singular-type peaks sitting on a flat background (see the three-dimensional profile of $q_{1,1}$ in Figures 1–4). This kind of solution is a singular soliton: it blows up at a specific point in the (x, t)-plane and decays quickly away from it. Families 1.2 and 1.3, by contrast, are built from $\tanh(\xi)$ and provide smoother, bell-shaped bright-soliton profiles that remain finite everywhere. The companion field $r_{1,2}$ in Family 1.2 displays a periodic array of acute peaks along the t-axis, which points to a spatially periodic soliton pattern rather than a single localized pulse. However, as noted above, these are non-propagating modes.

Effect of the free parameters. The parameter ρ, which comes from the existing constant in the given auxiliary equation, controls how close the solution sits to the singular limit: as $(\rho^2 - 1) \to 0$, several coefficients (for example, σ_0, θ_0, and k in Family 1.1) diverge, so ρ acts as a control knob between regular bright solitons and singular ones. The wave numbers k and l and the frequency ω set the slope and the speed of the wave peaks in the (x, y, t) space; changing l mainly rotates the wave front in the x-y plane, while ω mainly sets how quickly the waveform propagates in time, matching what the two-dimensional time-evolution plots show for $q_{1,1}$ (Figure 4), where increasing t shifts the peak location uniformly along x without modifying its height.

Amplitude and stability of the profiles. For the field $r_{2,1}$ (Family 2.1), showing mixed amplitudes (positive and negative real and imaginary parts) rather than a single decayed pulse, this solution behaves more like a kink or a periodic frontal than an isolated soliton. Its absolute value $|r_{2,1}|$ is kept bounded and forms a single ridge that travels at steady speed, which is a good sign of a stable traveling framework over the plotted domain $-10 \leq x \leq 10$, $0 \leq t \leq 10$, although as a non-propagating mode, it does not represent standard wave propagation.

Comparison with related models. These solution types (bright, singular, and periodic/kink-like) match what has been reported for the closely related Akbota and Kuralay equations, which supports the idea that the complex AMTZE belongs to the same structure family and exhibits similar soliton behavior, even though its extra spatial directions and higher-order cross-derivative term give it a more extensive set of free parameters to form.

On the method. The implemented method required only one reducing step (traveling wave transformation) and one balancing comparison to produce several independent, closed-form solution families. This confirms prior reports that the method scales well to paired, higher-order systems without extra manual work, and it eliminates the tedious accounting procedures that classical methods such as the Painlevé test or Hirota's bilinear method usually need for a q_{xxy}-type term.

Regarding the singular solutions. We acknowledge that the singular soliton solutions (Family 1.1) contain points where denominators vanish. From a mathematical perspective, these are valid weak solutions to the governing equations. From a physical standpoint, they represent idealized localized structures. Such singular solutions often appear in nonlinear wave theory and have been reported for many integrable systems. The singularities can be regularized by adding small perturbations or by considering the solutions in the sense of distributions.

Regarding imaginary frequencies. Some solution families (Families 1.2, 2.1–2.3) give imaginary values for ω. This means the wave variable $\xi = kx + ly - \omega t$ has an imaginary time component, leading to exponential growth or decay in time. While these are valid mathematical solutions to the reduced ODE, they represent non-propagating modes rather than standard traveling waves. Such solutions describe instability modes or transient phenomena in physical systems. For physically meaningful propagating waves, one should restrict to the families with real ω (such as Family 1.1).

6. Conclusions

We examined the complex AMTZE, a new triple integrable system built from a two-dimensional geometric spin model. We reduced it to one ODE with an appropriate traveling wave transformation. Then we solved that ODE with the modified generalized Kudryashov method, taking advantage of up-to-date software computation tools. We found six parameter families of exact solutions, split between a tanh-based branch and a coth rational branch. The obtained solutions include bright solitons, singular solitons, and periodic traveling waves. The free parameters ρ, k, l, and ω let us move smoothly between these shapes, which gives good control for anyone who wants to model a specific physical wave pattern. The results conform well with what is generally known about the closely associated Akbota and Kuralay equations, and they add new closed-form solutions to this expanding family. It is important to mention that all the obtained solutions have been confirmed as true. Each solution has been substituted for the main model and is fulfilled by software computation tools. It should be emphasized that among the six solution families, only Family 1.1 yields real frequencies ω and thus represents standard propagating traveling waves, while the remaining five families produce imaginary frequencies corresponding to non-propagating modes. This distinction is crucial for any physical interpretation of the results. Future work can look at the stability of these solutions, at their conservation laws, and at numerical checks against direct simulation of the original system.

Author contributions

Adnan Ahmad Mahmud: Conceptualization, writing-original draft, writing-review and editing, software; Akbota Myrzakul: Resources, validation, formal analysis, visualization, funding acquisition; Ratbay Myrzakulov: Supervision, investigation, methodology, validation; Hozan Hilmi: Conceptualization, methodology, investigation, formal analysis, visualization; Kalsum Abdulrahman Muhamad: Investigation, methodology, project administration, funding acquisition, visualization; Gulgassyl Nugmanova: Formal analysis, data curation, investigation, validation, recourse. All authors have read and approved the final version of the manuscript.

Use of Generative-AI tools declaration

The authors declare they have not used Artificial Intelligence (AI) tools in the creation of this article.

Acknowledgments

This work was supported by the Ministry of Science and Higher Education of the Republic of Kazakhstan, Grant No: AP22683222.

Conflict of interest

The authors indicate that there is no conflict of interest.

References

1. R. Myrzakulov, S. Vijayalakshmi, R. N. Syzdykova, M. Lakshmanan, On the simplest (2+1)-dimensional integrable spin systems and their equivalent nonlinear Schrödinger equations, *J. Math. Phys.*, **39** (1998), 2122–2139. https://doi.org/10.1063/1.532279
2. R. Myrzakulov, S. Vijayalakshmi, G. N. Nugmanova, M. Lakshmanan, A (2+1)-dimensional integrable spin model: Geometrical and gauge equivalent counterpart, solitons and localized coherent structures, *Phys. Lett. A*, **233** (1997), 391–396. https://doi.org/10.1016/S0375-9601(97)00457-X
3. Z. Sagidullayeva, G. Nugmanova, R. Myrzakulov, N. Serikbayev, Integrable Kuralay equations: Geometry, solutions and generalizations, *Symmetry*, **14** (2022), 1374. https://doi.org/10.3390/sym14071374
4. Z. Sagidullayeva, K. Yesmakhanova, N. Serikbayev, G. Nugmanova, K. Yerzhanov, R. Myrzakulov, Integrable Zhaidary equations: Reductions and gauge equivalence, *arXiv:2205.02073*, 2026. https://doi.org/10.48550/arXiv.2205.02073
5. K. A. Rashedi, M. Y. Almusawa, H. Almusawa, T. S. Alshammari, A. Almarashi, Applications of Riccati-Bernoulli and Bäcklund methods to the Kuralay-II system in nonlinear sciences, *Mathematics*, **13** (2025), 84. https://doi.org/10.3390/math13010084
6. A. Arshad, M. W. Yasin, I. Saeed, N. Ahmed, E. Bittaye, M. Z. Baber, Optical closed form soliton structures for the Kuralay-ii equation in nonlinear optical complex media, *Sci. Rep.*, **15** (2025), 37938. https://doi.org/10.1038/s41598-025-05073-2
7. W. A. Faridi, M. A. Bakar, Z. Myrzakulova, R. Myrzakulov, M. Elamin, L. Ragoub, et al., The construction of analytical exact soliton waves of Kuralay equation, *Acta Mech. Autom.*, **18** (2024), 603–615. https://doi.org/10.2478/ama-2024-0064
8. J. Liu, Z. Li, Bifurcation analysis and soliton solutions to the Kuralay equation via dynamic system analysis method and complete discrimination system method, *Qual. Theory Dyn. Syst.*, **23** (2024), 126. https://doi.org/10.1007/s12346-024-00990-5
9. S. H. Alfalqi, M. M. A. Khater, Numerical solutions and analytical methods for the Kuralay equation: A path to understanding integrable systems, *Opt. Quant. Electron.*, **56** (2024), 756. https://doi.org/10.1007/s11082-024-06597-z
10. T. Mathanaranjan, Optical soliton, linear stability analysis and conservation laws via multipliers to the integrable Kuralay equation, *Optik*, **290** (2023), 171266. https://doi.org/10.1016/j.ijleo.2023.171266
11. S. Kumar, N. Mann, Dynamic study of qualitative analysis, traveling waves, solitons, bifurcation, quasiperiodic, and chaotic behavior of integrable Kuralay equations, *Opt. Quant. Electron.*, **56** (2024), 859. https://doi.org/10.1007/s11082-024-06701-3

12. A. Zafar, M. Raheel, M. R. Ali, Z. Myrzakulova, A. Bekir, R. Myrzakulov, Exact solutions of M-fractional Kuralay equation via three analytical schemes, *Symmetry*, **15** (2023), 1862. https://doi.org/10.3390/sym15101862

13. E. H. M. Zahran, Z. Umurzakhova, A. Bekir, R. Myrzakulov, R. A. Ibrahim, New diverse types of the soliton arising from the integrable Kuralay equations against its numerical solutions, *Eur. Phys. J. Plus*, **139** (2024), 974. https://doi.org/10.1140/epjp/s13360-024-05765-0

14. T. Mathanaranjan, R. Myrzakulov, Integrable Akbota equation: Conservation laws, optical soliton solutions and stability analysis, *Opt. Quant. Electron.*, **56** (2024), 564. https://doi.org/10.1007/s11082-023-06227-0

15. H. Y. Kong, R. Guo, Dynamic behaviors of novel nonlinear wave solutions for the Akbota equation, *Optik*, **282** (2023), 170863. https://doi.org/10.1016/j.ijleo.2023.170863

16. W. A. Faridi, M. A. Bakar, M. B. Riaz, Z. Myrzakulova, R. Myrzakulov, A. M. Mostafa, Exploring the optical soliton solutions of Heisenberg ferromagnet-type of Akbota equation arising in surface geometry by explicit approach, *Opt. Quantum Electron.*, **56** (2024), 1046. https://doi.org/10.1007/s11082-024-06904-8

17. M. Awadalla, A. Taishiyeva, R. Myrzakulov, J. Alahmadi, A. A. Zaagan, A. Bekir, Exact analytical soliton solutions of the m-fractional Akbota equation, *Sci. Rep.*, **14** (2024), 13360. https://doi.org/10.1038/s41598-024-64328-6

18. S. S. Mahmood, S. M. Boulaaras, M. A. S. Murad, S. Malik, Optical solutions to the time fractional akbota equation arising in nonlinear optics via two distinct methods, *Sci. Rep.*, **15** (2025), 28823. https://doi.org/10.1038/s41598-025-14719-0

19. R. A. Ibrahim, A. Bekir, E. H. M. Zahran, On the exact traveling wave solutions to the Akbota-Gudekli-Kairatzhaidary equation and its numerical solutions, *Eur. Phys. J. Plus*, **140** (2025), 354. https://doi.org/10.1140/epjp/s13360-025-06289-x

20. E. H. Zahran, A. Bekir, R. A. Ibrahim, R. Myrzakulov, The new soliton solution types to the Myrzakulov-Lakshmanan-XXXII-equation, *AIMS Mathematics*, **9** (2024), 6145–6160. https://doi.org/10.3934/math.2024300

21. Z. Myrzakulova, S. Manukure, R. Myrzakulov, G. Nugmanova, Integrability, geometry and wave solutions of some Kairat equations, *arXiv:2307.00027*, 2025. https://doi.org/10.48550/arXiv.2307.00027

22. W. A. Faridi, G. H. Tipu, M. B. Riaz, A. M. Mostafa, S. A. AlQahtani, R. Myrzakulov, et al., Analyzing optical soliton solutions in Kairat-X equation via new auxiliary equation method, *Opt. Quant. Electron.*, **56** (2024), 1317. https://doi.org/10.1007/s11082-024-07197-7

23. A. A. Mahmud, T. Tanriverdi, K. A. Muhamad, Exact traveling wave solutions for (2+1)-dimensional Konopelchenko-Dubrovsky equation by using the hyperbolic trigonometric functions methods, *Int. J. Math. Comput. Eng.*, **1** (2023), 11–24. https://doi.org/10.2478/ijmce-2023-0002

24. M. Iqbal, D. Lu, A. R. Seadawy, F. A. H. Alomari, Z. Umurzakhova, R. Myrzakulov, Constructing the soliton wave structure to the nonlinear fractional Kairat-X dynamical equation under computational approach, *Mod. Phys. Lett. B*, **39** (2025), 2450396. https://doi.org/10.1142/S0217984924503962

25. A. M. Wazwaz, Extended (3+1)-dimensional Kairat-II and Kairat-X equations: Painlevé integrability, multiple soliton solutions, lump solutions, and breather wave solutions, *Int. J. Numer. Methods Heat Fluid Flow*, **34** (2024), 2177–2194. https://doi.org/10.1108/HFF-01-2024-0053

26. S. T. Demiray, H. Bulut, E. Celik, Soliton solutions of Wu-Zhang system by generalized Kudryashov method, *AIP Conf. Proc.*, **2037** (2018), 020025. https://doi.org/10.1063/1.5078480

27. M. Eslami, H. Rezazadeh, The first integral method for Wu-Zhang system with conformable time-fractional derivative, *Calcolo*, **53** (2016), 475–485. https://doi.org/10.1007/s10092-015-0158-8

28. A. A. Mahmud, K. A. Muhamad, T. Tanriverdi, H. M. Baskonus, Analyzing soliton dynamics of the solutions of (3+1)-dimensional Gardner-Kadomtsev-Petviashvili model for pulse propagation in single-mode optical fibers, *Z. Angew. Math. Phys.*, **77** (2026), 141. https://doi.org/10.1007/s00033-026-02766-0

29. T. Tanriverdi, A. A. Mahmud, K. A. Muhamad, H. M. Baskonus, H. Menken, A study on the (2+1)-dimensional integro-differential Jaulent-Miodek equation, *Comput. Math. Math. Phys.*, **66** (2026), 489–505. https://doi.org/10.1134/S0965542525702124

30. A. A. Mahmud, K. A. Muhamad, T. Tanriverdi, Further characteristics for certain newly formed solutions for two significant mathematical models by utilization of an efficient semi-analytic method, *Int. J. Math. Comput. Eng.*, **4** (2026), 419–438. https://doi.org/10.2478/ijmce-2026-0022

31. A. A. Mahmud, K. A. Muhamad, T. Tanriverdi, Dynamical behavior and soliton solutions of the (2+1)-dimensional Novikov-Veselov system of equations, *Nonlinear Anal. Comput. Simul.*, **1** (2026), 1. https://doi.org/10.53941/nacs.2026.100001

32. A. A. Mahmud, H. Hilmi, K. A. Muhamad, An efficacious improvement of the Anuj transformation method for solving higher-order fractional differential equations with constant coefficients, *Math. Model. Control*, **6** (2026), 140–150. https://doi.org/10.3934/mmc.2026011

33. A. A. Mahmud, Considerable traveling wave solutions of the generalized Hietarinta-type equation, *Int. J. Math. Comput. Eng.*, **3** (2025), 185–200. https://doi.org/10.2478/ijmce-2025-0015

34. J. Yu, F. Yu, Non-autonomous soliton, wave propagation and collision dynamic for (2+1)-dimensional higher-order nonlinear Schrödinger equation with variable coefficients, *Appl. Math. Lett.*, **174** (2026), 109937. https://doi.org/10.1016/j.aml.2025.109827

35. K. Hosseini, P. Mayeli, D. Kumar, New exact solutions of the coupled sine-Gordon equations in nonlinear optics using the modified Kudryashov method, *J. Mod. Opt.*, **65** (2018), 361–364. https://doi.org/10.1080/09500340.2017.1380857

36. W. Razzaq, A. Zafar, H. M. Ahmed, W. B. Rabie, Construction of solitons and other wave solutions for generalized Kudryashov's equation with truncated M-fractional derivative using two analytical approaches, *Int. J. Appl. Comput. Math.*, **10** (2024), 21. https://doi.org/10.1007/s40819-023-01660-x

37. A. Azhikhan, G. Nugmanova, R. Myrzakulov, K. Yesmakhanova, Z. Myrzakul, The Kuralay-Ma-Myrzakulov equation and the Akbota–Myrzakulov-Tolkynay-Zhaidary equation: Integrability, equivalence, reductions, and solutions, *AIMS Mathematics*, **11** (2026), 18222–18240. https://doi.org/10.3934/math.2026741

38. S. S. Mahmood, M. A. S. Murad, Investigation of the soliton solutions, bifurcation analysis, and chaotic nature of the Akbota-Myrzakulov-Tolkynay-Zhaidary equation, *Commun. Theor. Phys.*, **78** (2026), 085002. https://doi.org/10.1088/1572-9494/ae6a79

39. M. Zhou, F. Yu, Space-time shifted solitons and solution interactions for a generalized nonlocal nonlinear Schrödinger equation, *Appl. Math. Lett.*, **178** (2026), 109937. https://doi.org/10.1016/j.aml.2026.109937

40. J. Liu, L. Li, F. Yu, M. Liu, Soliton solutions and long-time asymptotics for variable-coefficient Mel'nikov system, *Phys. Scr.*, **101** (2026), 155215. https://doi.org/10.1088/1402-4896/ae5bd3

41. C. Zhang, L. Li, F. Yu, Soliton interaction dynamic, long-time asymptotic, and modulation instability for variable-coefficient Davey-Stewartson II equation in nonlinear medium, *Eur. Phys. J. Plus*, **141** (2026), 544. https://doi.org/10.1140/epjp/s13360-026-07763-w

AIMS Press